RBE 502 — Robot Control Spring 2023

RBE 502 Final Project: Robust Trajectory Tracking for Quadrotor UAVs using Sliding Mode Control

Chinmayee Prabhakar

101177306

Uthiralakshmi Sivaraman

133545470

Introduction:

This project's main goal is to create a reliable and efficient control system that enables a quadrotor to accurately follow desired flight paths while mitigating external disturbances. Our research will focus on developing a control design tailored for the Crazyflie 2.0 platform, a micro air vehicle (MAV) quadrotor known for its compact size and lightweight construction.

Weighing just 27 grams and small enough to fit in the palm of your hand, the Crazyflie is an ideal platform for conducting indoor lab experiments without causing considerable damage to its surroundings. Despite its high RPM propellers, the quadrotor's soft blades and low-torque coreless DC-motors render it crash-tolerant when compared to brushless motor alternatives.

The Crazyflie 2.0 features four 7mm coreless DC-motors that provide enough thrust to achieve a maximum takeoff weight of 42 grams. This lightweight and maneuverable design allows for precision control and navigation in confined spaces, making it an excellent candidate for our proposed robust control scheme development. Through this project, we aim to enhance the capabilities of MAVs like the Crazyflie 2.0, improving their adaptability and utility in various applications.

RBE 502 - ROBOT CONTROL

Final Project: Robust Trajectory Tracking For Quadrotor UAVs using Sliding Mode Control

Generalized co-ordinates: $q = [x, y, z, \phi, \theta, \psi]^T$

$$q \in \mathbb{R}^6$$

Control Inputs: $u = [u_1, u_2, u_3, u_4]$

The desired rotor speeds ω_i:

$$\begin{bmatrix} \omega_1^2 \\ \omega_2^2 \\ \omega_3^2 \\ \omega_4^2 \end{bmatrix} = \begin{bmatrix} 1/4k_F & -\sqrt{2}/4k_F l & -\sqrt{2}/4k_F l & -1/4k_M k_F \\ 1/4k_F & -\sqrt{2}/4k_F l & \sqrt{2}/4k_F l & 1/4k_M k_F \\ 1/4k_F & \sqrt{2}/4k_F l & \sqrt{2}/4k_F l & -1/4k_M k_F \\ 1/4k_F & \sqrt{2}/4k_F l & -\sqrt{2}/4k_F l & 1/4k_M k_F \end{bmatrix} \begin{bmatrix} u_1 \\ u_2 \\ u_3 \\ u_4 \end{bmatrix}$$

Equations of Motion:

$$\ddot{x} = 1/m\,(\cos\phi \sin\theta \cos\psi + \sin\phi \sin\psi)\,u_1$$

$$\ddot{y} = 1/m\,(\cos\phi \sin\theta \sin\psi - \sin\phi \cos\psi)\,u_1$$

$$\ddot{z} = 1/m\,(\cos\phi \cos\theta)\,u_1 - g$$

$$\ddot{\phi} = \dot{\theta}\dot{\psi}\,\frac{I_y - I_z}{I_x} - \frac{I_p}{I_x}\Omega\dot{\theta} + \frac{1}{I_x}u_2$$

$$\ddot{\theta} = \dot{\phi}\dot{\psi}\,\frac{I_z - I_x}{I_y} + \frac{I_p}{I_y}\Omega\dot{\phi} + \frac{1}{I_y}u_3$$

$$\ddot{\psi} = \dot{\phi}\dot{\theta}\,\frac{I_x - I_y}{I_z} + \frac{1}{I_{yz}}u_4$$

1 Trajectory Generation

A quintic polynomial of the fifth order is established for each coordinate (x, y, and z) in the given scenario. The trajectory is divided into five distinct segments by the provided five waypoints. For each segment, initial and final conditions are specified, leading to the creation of a series of linear equations upon substitution of these conditions.
Subsequently, the coefficients of the polynomials are determined by solving the resulting linear equations.

By utilizing this method, we can generate smooth and continuous trajectories, ensuring that the motion is adequately controlled throughout the entire path. The quintic polynomial approach enables the calculation of higher-order derivatives such as velocity, acceleration, and jerk, which are essential for optimizing the performance and stability of the control system. This approach also allows for easy modification of trajectories in real-time, adapting to changing requirements or environmental conditions.

Overall, the implementation of quintic polynomials for trajectory planning provides a robust and versatile foundation for developing advanced control schemes in various applications, including robotics, automation, and autonomous vehicle navigation.

Part - 1 : The position, velocity and acceleration trajectories for the translational co-ordinates (x, y, z)

Quintic Polynomial Trajectories:

$$q(t) = a_0 + a_1 t + a_2 t^2 + a_3 t^3 + a_4 t^4 + a_5 t^5$$

$$\dot{q}(t) = a_1 + 2a_2 t + 3a_3 t^2 + 4a_4 t^3 + 5a_5 t^4$$

$$\ddot{q}(t) = 2a_2 + 6a_3 t + 12a_4 t^2 + 20a_5 t^3$$

Deriving the eqs & constraints:

A

						a		b
1	t_0	t_0^2	t_0^3	t_0^4	t_0^5	a_0		q_{t_0}
0	1	$2t_0$	$3t_0^2$	$4t_0^3$	$5t_0^4$	a_1		$\dot{q}_{t_0}$
0	0	2	$6t_0$	$12t_0^2$	$20t_0^3$	a_2	=	$\ddot{q}_{t_0}$
1	t_f	t_f^2	t_f^3	t_f^4	t_f^5	a_3		q_{t_f}
0	1	$2t_f$	$3t_f^2$	$4t_f^3$	$5t_f^4$	a_4		$\dot{q}_{t_f}$
0	0	2	$6t_f$	$12t_f^2$	$20t_f^3$	a_5		$\ddot{q}_{t_f}$

Part 2 : Control Affine Form

$$\begin{bmatrix} \ddot{x} \\ \ddot{y} \\ \ddot{z} \\ \ddot{\phi} \\ \ddot{\theta} \\ \ddot{\psi} \end{bmatrix} = \begin{bmatrix} 0 \\ 0 \\ -g \\ \dot{\theta}\dot{\psi}\frac{I_y - I_z}{I_x} - \frac{I_p}{I_x}\Omega\dot{\theta} \\ \dot{\phi}\dot{\psi}\frac{I_z - I_x}{I_y} + \frac{I_p}{I_y}\Omega\dot{\phi} \\ \dot{\phi}\dot{\theta}\frac{I_x - I_y}{I_z} \end{bmatrix} + \begin{bmatrix} \frac{1}{m}(\cos\phi\sin\theta\cos\psi + \sin\phi\sin\psi) & 0 & 0 & 0 \\ \frac{1}{m}(\cos\phi\sin\theta\sin\psi - \sin\phi\cos\psi) & 0 & 0 & 0 \\ \frac{1}{m}(\cos\phi\cos\theta) & 0 & 0 & 0 \\ 0 & \frac{1}{I_x} & 0 & 0 \\ 0 & 0 & \frac{1}{I_y} & 0 \\ 0 & 0 & 0 & \frac{1}{I_z} \end{bmatrix} \begin{bmatrix} u_1 \\ u_2 \\ u_3 \\ u_4 \end{bmatrix}$$

$(\ddot{q})$ $f(q, \dot{q})$ $g(q, \dot{q})$

Plot of Desired Trajectories:

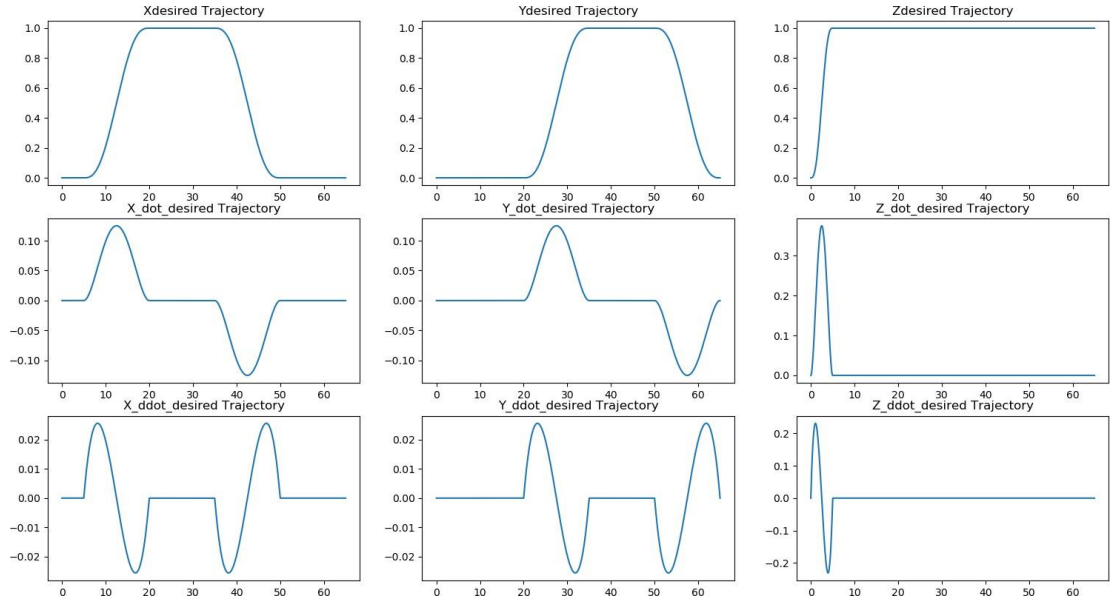

The above plots effectively illustrate the desired trajectories in 3D space, highlighting the smooth, continuous paths generated by the quintic polynomial method for each coordinate (x, y, and z), and their corresponding first and second derivatives.

2.1 Control Law Derivation and Altitude Estimation Z

Sliding mode control (SMC) is a powerful nonlinear control technique that has gained significant attention in recent years due to its robustness against system uncertainties, disturbances, and parameter variations. A key aspect of sliding mode control is the design of a sliding surface, which represents the desired system behavior. By driving the system to the sliding surface and maintaining it there, the control objective is achieved, and the system's performance is improved. One of the main advantages of SMC is its ability to handle errors effectively. When the system is operating on the sliding surface, errors between the actual and desired states are driven to zero, ensuring that the system's performance converges to the desired target. This strong convergence property makes SMC highly effective in dealing with errors, resulting in improved stability and precision of the controlled system.
Additionally, the robustness of SMC ensures that even in the presence of disturbances or uncertainties, the error remains bounded, providing a reliable and efficient control strategy for a wide range of applications.

This below image shows the design of the sliding surface equation:

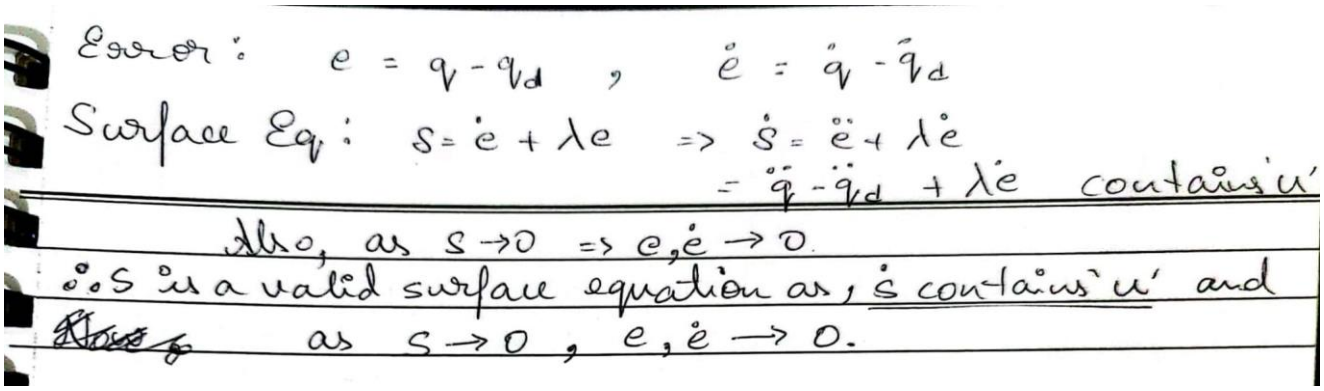

2.1 Control Law Derivation for 'z' attribute

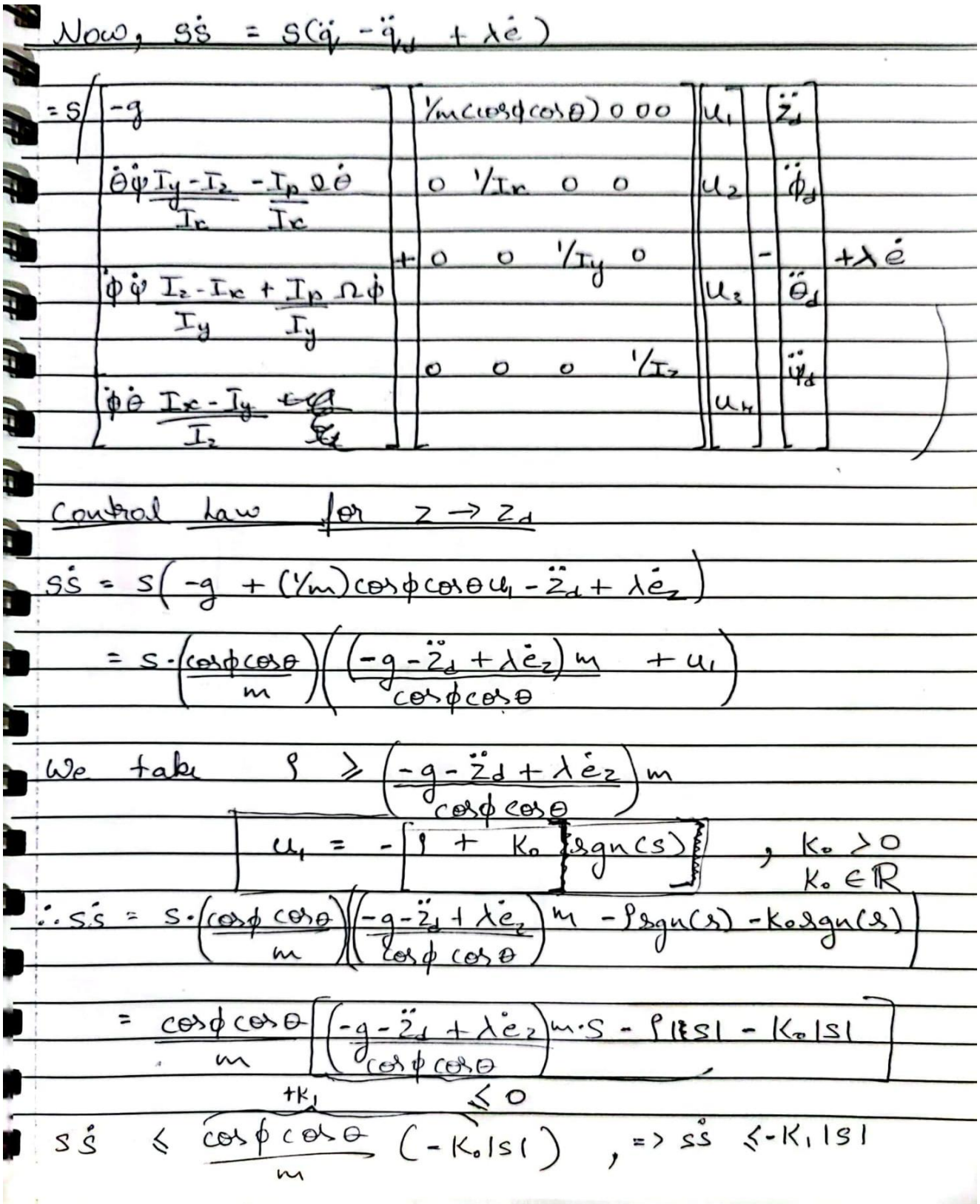

2.1 Control Law Derivation and Attitude Estimation (Roll, Pitch and Yaw)

Control law for $\phi \to \phi_d$:

$$s\dot{s} = s\cdot\left(\left[\dot{\theta}\dot{\psi}\frac{I_y - I_z}{I_x} - \frac{I_p\Omega\dot{\theta}}{I_x}\right] + \left(\tfrac{1}{I_x}\right)u_2 - \ddot{\phi}_d + \lambda\dot{e}_\phi\right)$$

$$= \frac{s}{I_x}\left(\dot{\theta}\dot{\psi}I_y - I_z - I_p\Omega\dot{\theta} + u_2 - \ddot{\phi}_d I_x + \lambda\dot{e}_\phi I_x\right)$$

We take, $\rho \geq \dot{\theta}\dot{\psi}I_y - I_z - I_p\Omega\dot{\theta} - \ddot{\phi}_d^{I_x} + \lambda\dot{e}_\phi I_x$

$$\boxed{u_2 = -\left[\rho + K_0\right]\operatorname{sgn}(s)}, \qquad K_0 > 0,\ K_0 \in \mathbb{R}$$

$$\therefore s\dot{s} = \frac{s}{I_x}\left(\dot{\theta}\dot{\psi}I_y - I_z - I_p\Omega\dot{\theta} - \ddot{\phi}_d^{I_x} + \lambda\dot{e}_\phi^{I_x} - \left[\rho + K_0\right]\operatorname{sgn}(s)\right)$$

$$= \frac{1}{I_x}\left(\underbrace{s\left(\dot{\theta}\dot{\psi}I_y - I_z - I_p\Omega\dot{\theta} - \ddot{\phi}_d^{I_x} + \lambda\dot{e}_\phi^{I_x}\right)}_{\leq 0} - \rho|s| - K_0|s|\right)$$

$$\Rightarrow s\dot{s} \leq -\frac{K_0}{I_x}|s| \Rightarrow s\dot{s} \leq -K_1|s|, \text{ where } K_1 = \frac{+K_0}{I_x}$$

Control law for $\theta \to \theta_d$:

$$s\dot{s} = s\left(\left[\frac{\dot{\phi}\dot{\psi}I_2 - I_x}{I_y} + \frac{I_p\Omega\dot{\phi}}{I_y}\right] + (1/I_y)u_2 - \ddot{\theta}_d + \lambda\dot{e}_\theta\right)$$

$$= \frac{s}{I_y}\left(\dot{\phi}\dot{\psi}I_2 - I_x + I_p\Omega\dot{\phi} + u_2 - \ddot{\theta}_d I_y + \lambda\dot{e}_\theta I_y\right)$$

* We take, $\rho \geq \dot{\phi}\dot{\psi}I_2 - I_x + I_p\Omega\dot{\phi} - \ddot{\theta}_d I_y + \lambda\dot{e}_\theta I_y$

$$\boxed{u_2 = -\left[\rho + k_0\right]\operatorname{sgn}(s)} \quad , \; k_0 > 0, \; k_0 \in \mathbb{R}$$

$$\therefore s\dot{s} = \frac{s}{I_y}\left(\dot{\phi}\dot{\psi}I_2 - I_x + I_p\Omega\dot{\phi} - \left[\rho + k_0\right]\operatorname{sgn}(s) - \ddot{\theta}_d I_y + \lambda\dot{e}_\theta I_y\right)$$

$$= \frac{1}{I_y}\left(\left(\dot{\phi}\dot{\psi}I_2 - I_x + I_p\Omega\dot{\phi} - \ddot{\theta}_d I_y + \lambda\dot{e}_\theta I_y\right)s - \left[\rho + k_0\right]|s|\right)$$

$$= \frac{1}{I_y}\left(\underbrace{\left(\dot{\phi}\dot{\psi}I_2 - I_x + I_p\Omega\dot{\phi} - \ddot{\theta}_d I_y + \lambda\dot{e}_\theta I_y\right)s}_{\leq 0} - \rho|s| - k_0|s|\right)$$

$$s\dot{s} \leq -\frac{k_0}{I_y}|s|$$

$$\Rightarrow s\dot{s} \leq -k_1|s| \quad , \text{ where } k_1 = \frac{k_0}{I_y}$$

Control law for $\psi \to \psi_d$

$$s\dot{s} = s\left[\frac{\dot{\phi}\dot{\theta}(I_x - I_y)}{I_z} + \frac{1}{I_z}\cdot u_4 - \ddot{\psi}_d + \lambda \dot{e}_\psi\right]$$

$$= s\cdot\frac{1}{I_z}\left[\dot{\phi}\dot{\theta}(I_x - I_y) - \ddot{\psi}_d I_z + \lambda \dot{e}_\psi I_z + u_4\right]$$

we take, $\rho \geq \dot{\phi}\dot{\theta}(I_x - I_y) - \ddot{\psi}_d I_z + \lambda \dot{e}_\psi I_z$

$$\therefore \boxed{u_4 = -[\rho + K_0]\,\mathrm{sgn}(s)}, \quad K_0 \geq 0, \; K_0 \in \mathbb{R}$$

$$\therefore s\dot{s} = \frac{s}{I_z}\left[\dot{\phi}\dot{\theta}(I_x - I_y) - \ddot{\psi}_d I_z + \lambda \dot{e}_\psi I_z - [\rho + K_0]\,\mathrm{sgn}(s)\right]$$

$$= \frac{\rho}{I_z}\left[\underbrace{\left(\dot{\phi}\dot{\theta}(I_x - I_y) - \ddot{\psi}_d I_z + \lambda \dot{e}_\psi I_z\right)}_{\leq \rho} s - \rho|s| - K_0|s|\right]$$

$$\Rightarrow s\dot{s} \leq \frac{-K_0}{I_z}|s| \quad \Rightarrow s\dot{s} \leq -K_1|s|$$

where $K_1 = \frac{K_0}{I_z}$

~~Boundary Layer~~

Since we are implementing a sliding mode control law with a boundary layer:

we replace the $\mathrm{sgn}(s)$ function with the $\mathrm{sat}\left(\frac{s}{\phi}\right)$ function

where sgn(s) is defined as:

if $s \geq 0$:

$sgn(s) = +1$

if $s < 0$,

$sgn(s) = -1$

sat(s/ϕ) is defined as:

if $|s| \geq \phi$, where $\phi \rightarrow$ boundary layer.

$sat(s/\phi) = sgn(s)$

if $|s| < \phi$, inside the boundary layer,

$sat(s/\phi)$

Therefore, the control laws are obtained as follows:

$$u_1 = \left[g - \lambda_1(\dot{z} - \dot{z}_d) + \ddot{z}_d - K_1\, sat(s_1/\phi)\right] \frac{m}{\cos\phi\cos\theta}$$

$$u_2 = \left[-\dot{\theta}\dot{\psi}\frac{I_y - I_z}{I_x} + \frac{I_p}{I_x}\Omega\dot{\theta} - \lambda_2\dot{\phi} - K_2\, sat(s_2/\phi)\right] I_x$$

$$u_3 = \left[-\dot{\phi}\dot{\psi}\frac{I_z - I_x}{I_y} + \frac{I_p}{I_y}\Omega\dot{\phi} - \lambda_3\dot{\theta} - K_3\, sat(s_3/\phi)\right] I_y$$

$$u_4 = \left[-\dot{\phi}\dot{\theta}\frac{I_x - I_y}{I_z} - \lambda_4\dot{\psi} - K_4\, sat(s_4/\phi)\right] I_z$$

3. Designing Parameters and Tuning Parameters

Given Parameters:

Parameter	Value
g	9.81 m/s²
m	0.027 kg
l	46mm
I_x	16.571710e-6 kg·m²
I_y	16.571710e-6 kg·m²
I_z	29.261652e-6 kg·m²,
I_p	12.65625e-8 kg·m².
K_f	1.28192e-8 N·m
K_m	5.964552e-3 N·m
W_{max}	2618 rad/s
W_{min}	0 rad/s

The given parameters represent the physical and control properties of a quadrotor system. The gravitational acceleration, g, is set to 9.81 m/s². The mass of the quadrotor, m, is 0.027 kg, and the distance between the center of mass and the propeller, l, is 46 mm.

The moments of inertia for the quadrotor along the x, y, and z axes are Ix = 16.571710e-6 kg·m², Iy = 16.571710e-6 kg·m², and Iz = 29.261652e-6 kg·m², respectively. The rotor moment of inertia, Ip, is 12.65625e-8 kg·m². The thrust and torque constants for the propellers are kF = 1.28192e-8 N·m and kM
= 5.964552e-3 N·m, respectively.

The maximum and minimum angular velocities for the propellers are w_max = 2618 rad/s and w_min =0 rad/s.

Tuned Parameters:

Parameters	Values
λ_z	5
λ_{phi}	12
λ_{theta}	12
λ_{psi}	5
K_{0z}	10
K_{0phi}	140
K_{0theta}	135
K_{0psi}	25
Φ	1
K_p	120
K_d	8

The control gains for the roll, pitch, yaw, and altitude are defined as lamda_phi = 12, lamda_theta = 12,

lamda_psi = 5, and lamda_z = 5. The initial control gains for the roll, pitch, yaw, and altitude are set to K0_phi = 140, K0_theta = 135, K0_psi = 25, and K0_z = 10. Additionally, the phi parameter is set to 1.

Lastly, the proportional and derivative gains for the control system are defined as kp = 120 and kd = 8. These values are essential in tuning the quadrotor's response to achieve the desired performance characteristics and ensure stable flight.

4. Plot of Desired vs Estimated Trajectories

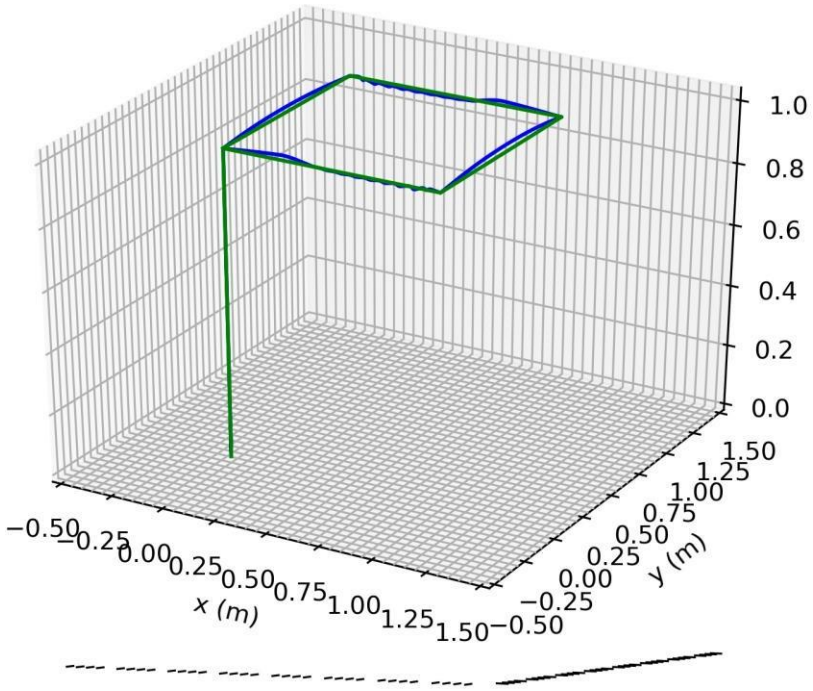

5. Part 3 Code Explanation

We obtain the desired trajectories of x,y,z defined in part 1, as well as calculate the desired trajectory of theta and psi using the equations described in the problem statement. We define the angular velocities of the motors equations as well as the control laws established in part 2. We evaluate the control laws and use it to compute the angular velocities for the drone.

6. Discussion and Conclusion

The 3D plot of the actual trajectory compared to the desired trajectory is depicted in Figure above. Upon analyzing the performance of the quadrotor, several observations can be made:

1. In the x-direction, the quadrotor exhibits a wobbling motion as it approaches the waypoint. Although there is a minor deviation from the planned trajectory, this discrepancy is minimal and does not significantly affect the overall performance.

2. In the y-direction, the quadrotor's movement is smooth, with only a slight overshot from the intended trajectory. Despite this, the tracking error remains negligible, indicating good adherence to the path.

3. As for the z-direction, the controller demonstrates excellent performance, ensuring accurate trajectory tracking and stable operation.

In conclusion, the quadrotor's overall performance in following the desired trajectory is commendable. While there are minor deviations in the x and y directions, these discrepancies are negligible and do not compromise the quadrotor's ability to reach its destination. The controller's performance in the z-direction is particularly noteworthy, as it maintains precise control of the quadrotor's altitude. These results suggest that the implemented control system is effective and reliable, enabling the quadrotor to execute complex flight paths with minimal error. Future work could involve refining the control algorithms or incorporating additional sensors to further improve trajectory tracking accuracy and stability.